Open access • Journal Article • DOI:10.1515/EPOLY.2012.12.1.507

Morphology, thermal properties and mechanical relaxations of metallocene syndiotactic polypropylenes — Source link

Ester López Moya, José M. Gómez-Elvira, Rosario Benavente, Ernesto Pérez

Institutions: Spanish National Research Council

Published on: 01 Dec 2012 - E-polymers (European Polymer Federation)

Topics: Molar mass and Tacticity

e-Polymers **2012**, no. 043

http://www.e-polymers.org

ISSN 1618-7229

Morphology, thermal properties and mechanical relaxations of metallocene syndiotactic polypropylenes

Ester López Moya, José M. Gómez-Elvira[*]*, Rosario Benavente, Ernesto Pérez*

Instituto de Ciencia y Tecnología de Polímeros, CSIC, Juan de la Cierva 3, 28006 Madrid, Spain; tel.: +34915622900; fax: +34915644853; e-mail: elvira@ictp.csic.es

(Received: 01 April, 2011; published: 07 April, 2012)

Abstract: The complex polymorphic behaviour of four syndiotactic polypropylene (sPP) samples have been analysed by means of DSC and WAXD techniques. Two samples (sPP1, sPP2) were synthesised via metallocene polymerization by using the ansa-zirconocene $Ph_2C(Cp)(9\text{-}Flu)ZrCl_2$ as catalyst. Finally, two additional specimens with different molar masses (sPP1-Fr1, sPP1-Fr2) were prepared from the most syndiotactic sPP1 sample by temperature gradient extraction. The WAXD analysis shows that together with the orthorhombic form I, form II can coexist in a variable but small proportion depending on both the chain features and the processing conditions. The relative contribution of the disordered and the ordered types of form I is also dictated by molar mass, configurational microstructure as well as processing conditions. The observed changes in the thermal properties as measured by DSC and in the mechanic-dynamical relaxations of the samples, on slowing the crystallisation rate down, can be rationalised in terms of two concurrent processes, namely the perfection undergone by the crystals and the segregation of the amorphous phase.

Introduction

When the stereoselective polymerization of olefins was discovered in 1954, syndiotactic polypropylene (sPP) was considered only as a scientific curiosity because it showed unprofitable properties due to the low stereo-regularity of the macromolecules synthesized with Ziegler-Natta catalysts (1).

In the middle of 1980s, a rebirth of sPP was observed due to the possibility of obtaining this thermoplastic with the new single-site metallocene catalysts (2). Some of these new catalysts were highly syndiospecific and therefore suitable for producing very crystalline sPP with a high melting temperature. The physical and chemical properties of metallocene sPP resulted to be completely different from those ones presented by isotactic polypropylenes. In fact, they exhibit better toughness, greater heat stability, tear resistance, ductility, elasticity and transparency, among other advantages.

The reason for the aforementioned differences in the properties of both stereoisomers lies on the alternating position of methyl groups along the sPP macromolecules. Such specific configuration gives on the one hand, a high flexibility to the chain together with a high density in the molten state, providing a great resistance to large-scale molecular motions. These features account for a relatively low value of T_m as well as a low value of the maximum attainable degree of crystallinity and a slower rate of crystallization when compared with iPP.

On the other hand, syndiotacticity is in the grounds of a complex polymorphic behaviour which is characterized by up to four crystalline structures. They are known as I, II, III and IV, according to the nomenclature proposed by De Rosa et al. which is based on their relative stabilities (3-9). Form I is the most stable and corresponds to an orthorhombic packing of helices with a GGTT conformation. It can appear either as an ordered type when right- and left-handed chains alternate in the "ab" plane of the cell, or as a disordered type when the antichiral helices package randomly in the "ab" plane. Form II is metastable and corresponds to a different orthorhombic alignment of isochiral helices. It is favoured under high pressure processing and by configurational and compositional chain defects (10). Finally, forms III and IV are the less stable. The former corresponds also to an orthorhombic packing of chains but with a trans-planar conformation, and the latter is formed by a monoclinic packing of chains with a helical conformation ($T_6G_2T_2G_2$).

The mechanical performance of sPP depends on its crystalline morphology which, in turn, is dictated by the steroregularity and the molar mass of the chains. There are numerous structural studies on this relationship and, in particular, on the elastomeric behaviour which is one of its most outstanding features (11-16). Notwithstanding the exhaustive work done, the influence of the wide spectrum of crystalline structures on the chain dynamics of the sPP has been scarcely tackled.

This work aims to characterize thoroughly the semicrystalline morphology of a series of sPP samples with different molar masses and microstructures (Table 1), and to explore the influence of the crystalline structure present on the mechanical relaxations of the amorphous regions, as they are assessed by means of dynamic-mechanical analysis.

Results and discussion

The distinctive chain microstructure of the studied samples is collected in Table 1.

Tab. 1. Intrinsic viscosity (η) and configurational microstructure of the samples.

Sample	η(mL.g^{-1})	mmmm	mmmr	rmmr	mmrr	mmrm + rmrr	mrmr	rrrr	mrrr	mrrm
sPP1	364	0.0	0.0	2.5	3.0	2.3	0.0	86.4	4.5	1.2
sPP1-Fr1	356	0.0	0.0	1.5	3.0	2.2	0.0	85.8	5.1	2.3
sPP1-Fr2	316	0.0	0.0	1.5	2.9	2.1	0.0	85.0	8.5	0.0
sPP2	111	0.0	0.0	2.7	4.0	10.2	0.0	65.5	4.5	3.0

Structural characterization

The WAXD patterns at room temperature of the processed films are shown in Figure 1. A first general remark is that all sPP samples exhibit four main diffraction peaks at 12.2º, 15.8º, 20.5º and 24.5º, which belong to the disordered form I. This polymorph is characterized by chains in a helical conformation (GGTT) packed in a orthorhombic unit cell (17). The peaks are assigned to the reflection of the planes (200), (020), (121) and (400) in increasing order of angles. The lack of the diffraction peak at 2θ = 18.8º, corresponding to the reflection of plane (211) of the ordered form I, excludes the presence of this polymorph in the Q-processed samples in a measurable quantity. The disordered form I is well-known to appear preferentially in low syndiotactic samples or in samples quickly crystallized from the melt at low temperature (18).

A closer examination of the WAXD traces of the Q-samples reveals the presence of a shoulder at 2θ = 17º which is very conspicuous in the case of sample sPP2-Q. This diffuse diffraction on the right of the peak at 15.8º has been reported to correspond to the reflection of the (110) plane of the orthorhombic isochiral form II (18). Such polymorph appears in small amount, together with the disordered form I, in low-syndiotactic sPP (with [rrrr]=70-80 %) (10,11,19). Figure 1 shows that form II is present in the as-prepared quenched powder sPP2 sample, as it can be inferred from the shoulder at 17º. The comparison of the sPP2 WAXD pattern in the powdery state with those ones of the Q and S films evidences that the Q processing renders, together with the lowest crystallinity, an enhanced relative content of the kinetically favoured form II. When the crystallisation rate slows down on going from the Q to the S processing, the partial vanishing of the contribution at 17º, as well as the sharpening of the form I peaks, suggests that the crystalline phase undergoes a perfection process. These changes imply not only the increment of the crystals' average size but also the progressive transformation of form II into the more stable antichiral form I.

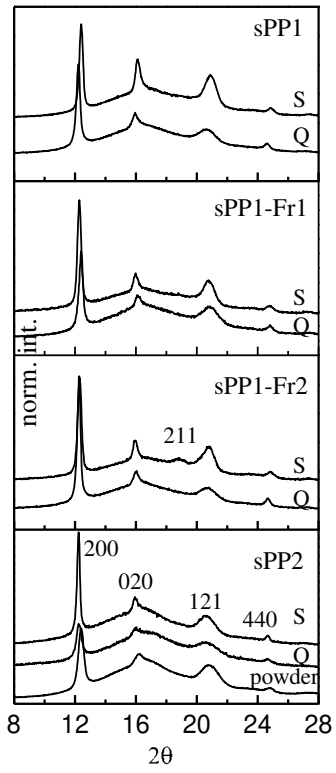

Fig. 1. X-ray Diffraction patterns, acquired at room temperature, of the indicated samples after 24 h annealing at ambient conditions.

The presence of form II can not be asserted in powdery sPP1, sPP1-Fr1 and sPP1-Fr2; however it appears in the Q-processed films and is negligible in the S-films (Figure 1). Additionally, there is a new peak at 18.8º in the S-processed samples sPP1-Fr1 and sPP1-Fr2 which reflects the presence of the ordered form I. This form is known to be favoured on crystallizing isothermally at high temperatures. In our

case, due to the moderately high syndiotacticity and rather low T_c values of sPP1, sPP1-Fr1 and sPP1-Fr2 (see below), the ordered form I is not strongly promoted and it is only detected in sPP1-Fr1 and sPP1-Fr2 which have a lower molar mass than sPP1. Anyway, the crystalline phase of the three highly syndiotactic samples seems to be also qualitatively improved in the S films by partially removing the structural disorder found in the Q-films, namely the disordered form I and the thermodynamically less stable form II.

As it was expected, the most amorphous polymer sPP2 does not exhibit the peak (211) either. The low stereoregularity of this sample prevents the perfect alternation of right and left-handed helices in the orthorhombic cell even under slow crystallization rates.

The crystalline contents obtained from the X-ray diffractograms are reported in Table 2. They are always higher in S-samples than in the corresponding Q-samples. The difference is clear for sPP1-Fr1 and sPP1-Fr2 samples but quite small in both the un-fractionated sPP1 and sPP2 polymers.

To get a deeper insight into the crystallization rate of the sPP specimens from the amorphous state, the sPP1-Fr2 and the sPP2 samples were selected as examples which are expected to behave in a different way because of both their characteristic microstructures and their molar masses. Both polymers were melted and quickly quenched at a suitable temperature. From such a completely disordered state, the crystalline growth was monitored by performing isothermal WAXD scans every few minutes in the case of sPP1-Fr2 and hours for sPP2.

In the case of fraction sPP1-Fr2, the molten polymer at 165 ºC was quenched at a temperature of 125 ºC which is remarkably below the T_m value measured by DSC.

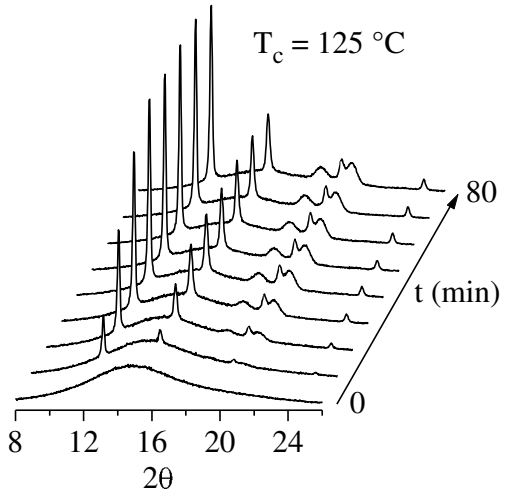

Fig. 2. Time evolution of the WAXD pattern of sPP1-Fr2 isothermally crystallized from the melt at 125 ºC. Only one every five frames has been plotted, for clarity of the presentation.

Figure 2 shows the time evolution of the diffractogram profile during 80 min. This period is large enough to achieve a maximum in the crystalline content. Actually, the kinetics of the crystalline growth can be monitored by means of the diffraction at 12.2º, which reflects a global measure of the ordered fraction, regardless of the

polymorph type. This is shown in Figure 3 where it can be appreciated that the area of such a peak reaches a maximum in 40 min, and no further crystallinity seems to be developed. The most remarkable feature is the appearance of the diffraction peak at 18.8º corresponding to the ordered form I. This higher ordering is also reflected on the relatively high degree of crystallinity developed by this specimen, which amounts to f_c^{WAXD} = 0.41, similar to that for sample sPP1-Fr2-S (see Table 2). Anyway, the crystals developed by isothermal crystallisation at 125 ºC seem to be more perfect, as deduced from the higher relative intensity of the peak at 18.8º and from the rather appreciable splitting of the diffractions around 20º.

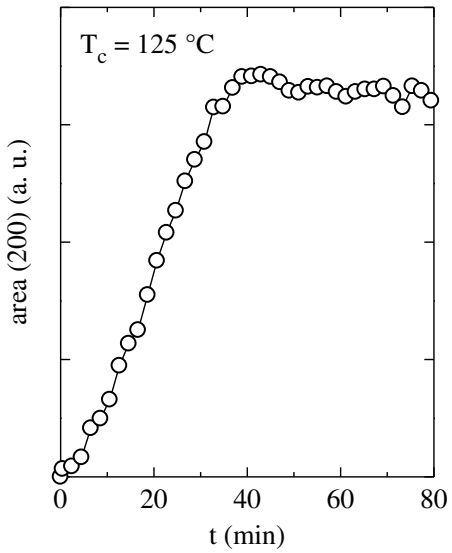

Fig. 3. Time evolution of the area of the (200) diffraction at 12.2º during the isothermal crystallization at 125 ºC of sample sPP1-Fr2.

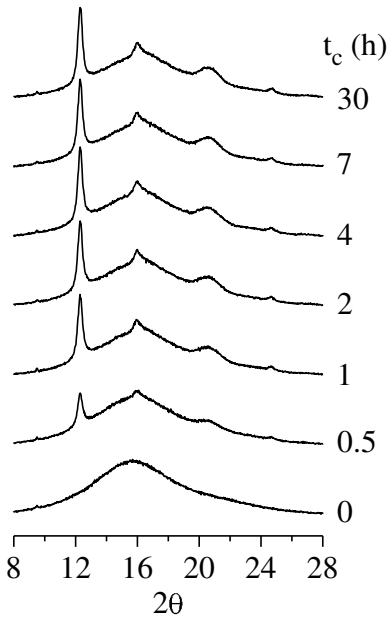

Fig. 4. Time evolution of the WAXD pattern of specimen sPP-Q isothermally crystallised from the melt at room temperature.

In the case of the sPP2 sample, the Q processing yields an actual amorphous state from which the isothermal crystalline growth at room temperature can be monitored. Figure 4 shows that the polymer develops a 0.08 wt% of crystallinity 30 min after the quenching, and almost the maximum crystalline level (0.17 wt.-%) in two hours. The peaks of the disordered form I appear from the beginning of the crystallization and only a very weak shoulder at 17º indicates the presence of the form II from 2 h onwards.

Tab. 2. Values of T_g, T_m, T_c and ΔH_m of sPP samples as measured by DSC: (F1) first melting scan; (F2) second melting scan. The crystalline content from the WAXD analysis is indicated as fc^{WAXD}, which is used to determine $\Delta H_m{}^{100WAXD}$.

Sample	$f_c{}^{WAXD}$	$T_g{}^{F1}$ (ºC)	$T_m{}^{F1}$ (ºC)	$\Delta H_m{}^{F1}$ (J/g)	$\Delta H_m{}^{100WAXD}$ (J/g)	T_c (ºC)	$T_g{}^{F2}$ (ºC)	$T_m{}^{F2}$ (ºC)	$\Delta H_m{}^{F2}$ (J/g)
sPP1-Q	0.31	5	140	51	165	89	0	140	47
sPP1-S	0.35	3	138	58	166	89	0	140	47
sPP1-Fr1-Q	0.31	9	138	53	171	86	0	139	43
sPP1-Fr1-S	0.38	3	139	59	155	86	0	139	43
sPP1-Fr2-Q	0.34	5	137	49	144	90	-1	139	47
sPP1-Fr2-S	0.42	5	142	65	155	90	-1	139	47
sPP2-Q	0.24	2	97	40	167	-	-1.5	99	2
sPP2-S	0.26	0	99	40	154	-	-1.5	99	2

Average value of $\Delta H_m{}^{100WAXD}$ = 159 ± 9 J/g

Thermal properties

The DSC curves of Q-processed samples are shown in Figure 5 and the values of the corresponding magnitudes are collected in Table 2.

In the first melting scan (Figure 5a), it is clear that a glass transition is present between 1 and 9 ºC. The lowest T_g value corresponds to sPP2-Q, which displays the most intense Cp change.

A second remark is the presence of a melting endotherm around 50 ºC which can be assigned to the annealing process undergone by the samples at room temperature. This crystalline growth takes place during the 24 h period elapsed between the processing and the first DSC run.

At temperatures higher than T_g, the imperfect crystals formed by quick cooling increase their size as far as the polymer dynamics let the segments join the primary crystalline structures. Furthermore, the secondary crystallization can also take place if new crystals are formed.

The high intensity of the melting peak at 50 ºC observed in sPP2-Q is consistent with this description. Actually, the most amorphous sample is expected to have the lowest crystallisation rate and, consequently, to yield a remarkable further annealing process at room temperature. The fact that the freshly prepared sPP2-Q sample is completely amorphous according to WAXD analysis, suggests that the melting endotherm at 50 ºC must be mostly attributed to isothermal crystallization (similar to the experiment in Figure 4) rather than to the perfection of primary crystals.

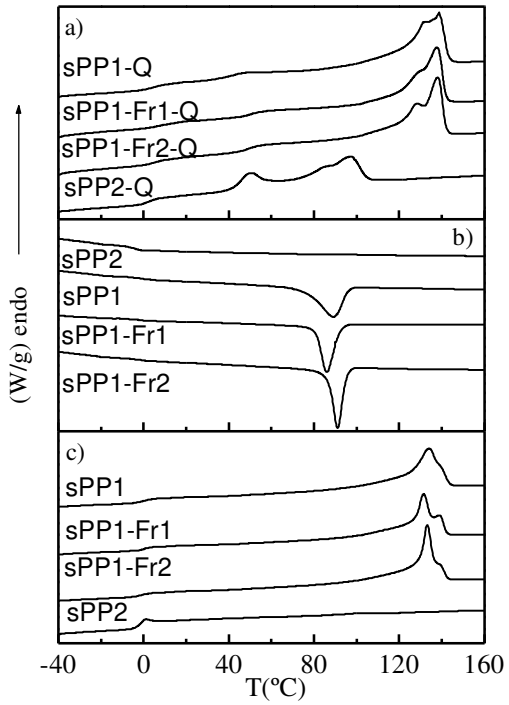

Fig. 5. DSC curves of the different sPP samples obtained by the Q processing: a) first DSC melting scan; b) DSC crystallization scan from the melt; c) second DSC melting scan. Scanning rate: 20 ºC/min.

In agreement with the aforementioned WAXD results, there is no evidence of any crystallization of the sPP2 sample by cooling the melt at 20 ºC/min (Figure 5b). On the contrary, the more syndiotactic Q-films (sPP1 and their fractions) indeed generate crystals when cooling the molten state even at relatively fast rates, as it is shown in Figure 5b. Then, the contribution of both the crystal perfection process and the generation of new low-T_m crystals at room temperature should be considered.
The melting endotherm at the highest temperature is always bimodal, showing a main peak at a T_m value between 97 ºC for sPP2-Q and 140 ºC for sPP1-Q. This feature must be ascribed to the occurrence of consecutive fusion-recrystallization-fusion processes, as for the WAXD analysis at variable temperature shows no other polymorph than the disordered form I. The endotherm's shape does not show the actual crystalline distribution of the samples because of the aforementioned dynamic evolution of the crystalline phase; however it reflects the chain features, i.e. molar mass and microstructure. Consequently, among the more syndiotactic samples, sPP1-FR2 shows the more conspicuous recrystallization process during the first DSC scan. This enhanced trend towards the perfection of crystals is in agreement with a slightly lower molar mass and a more regular stereostrucure (Table I).

The subsequent DSC runs of samples, cooled from the melt at 20 ºC/min (Figure 5c), show also the glass transition but at slightly lower temperatures (around 0 ºC). As in the first DSC melting scan, sample sPP2 evidences the most prominent Cp change due to its low crystallinity. In fact, the sample can be considered essentially amorphous because there is no crystalline development during the heating and a

melting endotherm is hardly apparent at about 90-100 ºC. Moreover, this reduced crystallinity leads to the observation of a small endothermic peak at the top of the glass transition in the second melting scan, arising from the enthalpic relaxation due to physical ageing (20, 21).

Concerning the second heating scan of sPP1, sPP1-Fr1 and sPP1-Fr2, the double melting process is the only feature apparent in these samples over T_g. Similarly to the case of the first DSC scan, such behaviour is also ascribed to the consecutive fusion-recrystallization-fusion processes. The most outstanding feature is the high intensity of the low-T_m peak at about 131ºC, relative to that one of the high-T_m peak at 140 ºC which appears as a shoulder. As it can be appreciated in Figure 5c, the lower the molar mass is, the higher the difference between peak intensities appears. It is well-known that the increase of the molar mass affects the crystallization kinetics and promotes the formation of less perfect crystals. Then, an increasing of the low-T_m crystalline fraction able to be improved through a fusion-recrystallization process is expected.

On the other hand, the crystalline content, as deduced from the enthalpy of melting, is in all samples lower than that one obtained from the first DSC scan (see Table 2), due to the absence of crystals generated by the annealing effect (or crystallization) at room temperature.

The thermal behaviour of sPP samples slowly cooled from the melt (S-samples) can be seen in Figure 6. These DSC curves show the glass transition at similar T_g values to those ones obtained in the case of Q-samples (Table 2). On the contrary, the main endotherm is not a double melting process but a single one. The generation of more perfect crystals in a slow process of crystallization (around 1.5 ºC/min) accounts for this fact.

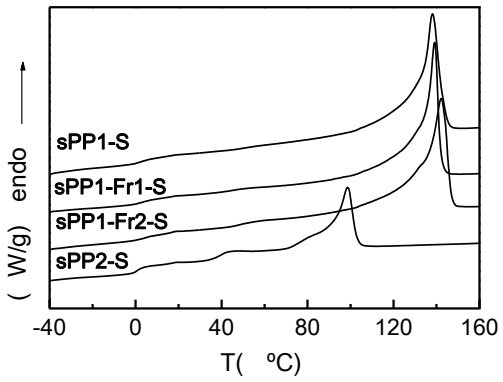

Fig. 6. First DSC melting traces of the sPP samples obtained by the S processing. Scanning rate: 20 ºC/min.

The crystallinities of S-samples (Table 2) turn out to be somewhat higher than the values obtained in the corresponding Q-samples, even though no significant annealing at room temperature is appreciated. The case of sPP2-S is an exception because it clearly shows a characteristic room temperature annealing shoulder around 40 ºC. The low crystallization rate of this sample and the low melting temperatures yield a solid state still far from the equilibrium, where chains can evolve above T_g giving rise to the commented secondary crystallization process.

Regarding the degrees of crystallinity deduced from the enthalpies of melting, a value of 196.6 J/g has been reported as the enthalpy of fusion of a perfect crystal of sPP (22). With this value, the DSC estimations of the crystallinity are systematically lower than those determined by WAXD. The reason may be just an overestimation of the enthalpy for perfect 100% crystallinity. In fact, if the actual values of the enthalpy of melting reported in Table 2 are taken together with the WAXD crystallinity, an average value of 159 ± 9 J/g is obtained for $\Delta H^{100\%\ WAXD}$ of sPP. This estimation appears to be more reasonable than the value of 196.6 J/g, especially when considering that $\Delta H^{100\%\ WAXD}$ for the α modification of iPP is reported to be in the interval from 162 to 169 J/g (23-25).

Mechanical properties

Figures 7 to 10 show plots of storage and loss moduli and tan δ as a function of temperature for the different samples with the two thermal treatments Q and S.

There is a controversy in the literature concerned to the number of relaxation processes existing in sPP. Similarly to the case of iPP, three characteristic mechanical relaxations, named α, β and γ in order of decreasing temperature, are found for sPP. As an example, Figure 7 shows the variation of tan δ and storage (E') and loss moduli (E") as a function of temperature for sample sPP1-Fr1(Q) at the two extreme frequencies used. The γ relaxation is detected as a smooth drop of E' at low temperature between -150 ºC to -50 ºC (Figure 7a). This relaxation appears as a peak in the temperature-dependent variations of tan δ and E'' (Figure 7b and 7c) and is generally attributed to local motions in the amorphous phase taking place at temperatures below T_g (26,27).

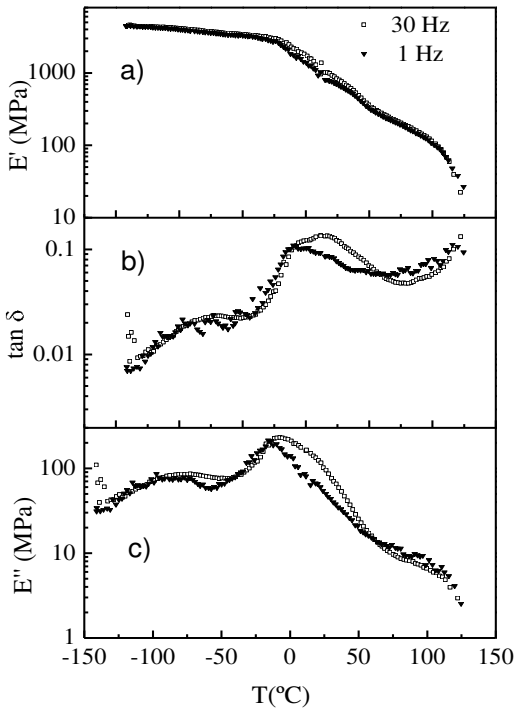

Fig. 7. Temperature dependence of a) storage (E') modulus, b) tan δ, and c) loss modulus (E'') of sPP1-Fr1-Q at the two extreme frequencies used.

The β relaxation, or glass transition, appears at the temperature at which cooperative motions begin in the amorphous regions of the polymer. The T_g value is typically around 0 ºC and is characterized by a sharp drop in E', which corresponds to a maximum in tan δ and E'' curves.

Finally, the existence of the α relaxation is still under discussion because it is a process not easily detected. According to Men et al (28), α motions would involve the crystalline phase, although the implication of restricted amorphous regions should not be ruled out. Arranz-Andrés et al (29) observed, in E", that the β relaxation is asymmetric in the higher temperature side, pointing out the overlapping of this cooperative movement with another more local motion. They conclude that α relaxation process related to a motion that involves crystalline regions, in some extent, is taking place, as occurred in iPP (30).

The results found in this study do not show a clear evidence of the α process at temperature above T_g. However, the E' drop associated to the glass transition is wide and featured by a very short plateau previous to a gentle drop on the high temperature side. This process is detected in E'' as a shoulder in the high temperature regions (or lower frequencies) of the β relaxation and could be related to movements either associated to the crystalline phase or to a somewhat constrained amorphous region. This is a topic which requires a more detailed study, because not only the quality of the amorphous phase but also the type of the crystalline polymorph could play an important role in the α relaxation characteristics.

The variations of E', E'' and tan δ with temperature, at 3 Hz as a representative example, are plotted in Figures 8, 9 and 10 respectively, for the different samples studied and for the two processing performed.

Tab. 3. Values of E' at 3 Hz for the sPP samples at -120 ºC and at 25 ºC.

Sample	E'-120ºC (MPa)	E' 25ºC (MPa)
sPP1-Q	3310	575
sPP1-S	3460	570
sPP1-Fr1-Q	4250	510
sPP1-Fr1-S	3980	630
sPP1-Fr2-Q	3630	530
sPP1-Fr2-S	3680	620
sPP2-Q	3350	255
sPP2-S	4600	290

Figures 9 shows the effect of the processing conditions on the mechanical relaxation characteristics, as they were measured by means of the temperature dependence of E''. A global examination of the E'' DMTA spectra allows to realize on the one hand, that the glass transition is not a single process and, on the other hand, that the S processing causes the relative intensity of the low-temperature component of the T_g to increase. This effect is apparent mainly in sPP2 specimen, where a remarkable shift of the T_g towards a low temperature value takes place.

This change in the characteristics of the β relaxation supports the idea suggested from the comparison of E" in Q and S films (Figure 9), namely the crystals undergo a perfection process as a consequence of slowing the cooling rate of the molten polymer down. Such a thermal history helps the segregation of phases to take place,

yielding an enhanced content of the amorphous phase broken away from crystals. The large T_g shifting in sPP2 is consistent with a particularly favoured perfection process which would account for the huge E' improvement shown under T_g. The change in the crystals' quality can be visibly appreciated in the sPP2 case which shows the highest E' change under T_g. Actually, the WAXD patterns of this sample in Figure 1 displayed the largest reduction in the content of the form II by performing the S processing instead of the Q one. This removal could be mostly in the basis of such an E' increment, since it is well known the ability of this polymorph to confer flexibility to the chains (10-16).

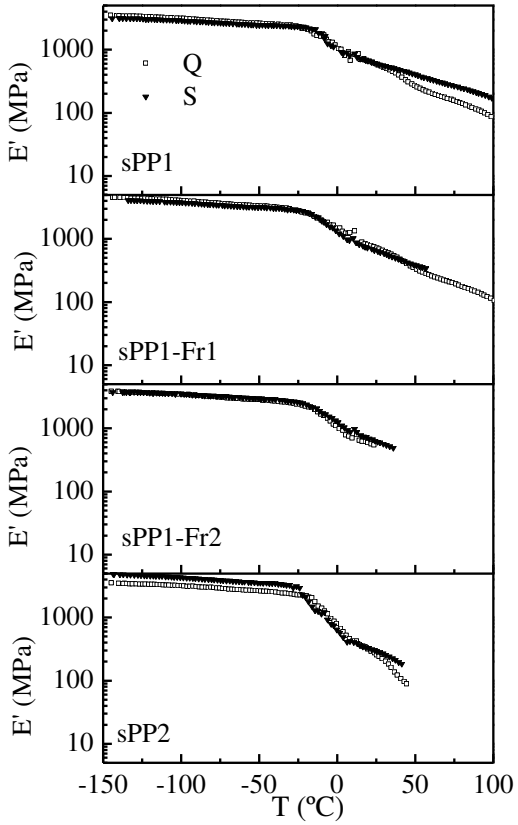

Fig. 8. Temperature-dependent variation of E' for the different sPP samples at 3 Hz.

The maxima of the β and γ relaxations are better resolved in the DMTA E'' spectrum (Figure 9) than in the tan δ one (Figure 10). Consequently, the data were taken from the E'' DMTA spectra to estimate the apparent E_{act} by fitting them to an Arrhenius relationship. T_γ and T_β values at 3 Hz as well as the E_{act} of both relaxations, calculated from the four frequencies used, are summarized in Table 4 (experimental error ± 25 kJ/mol).

The γ relaxation shows lower E_{act} values than the β relaxation, in agreement with data reported by other authors (29). Nevertheless, a significant difference between S and Q processed samples is generally appreciable in the case of the γ relaxation and in the β relaxation of two of the samples. Although the error in the assignment of the $T\gamma_{max}$ is large, differences in $E_{act}(\gamma)$ of Q and S samples are reliable and could reflect the influence of the semi-crystalline morphology on the motions of the amorphous phase.

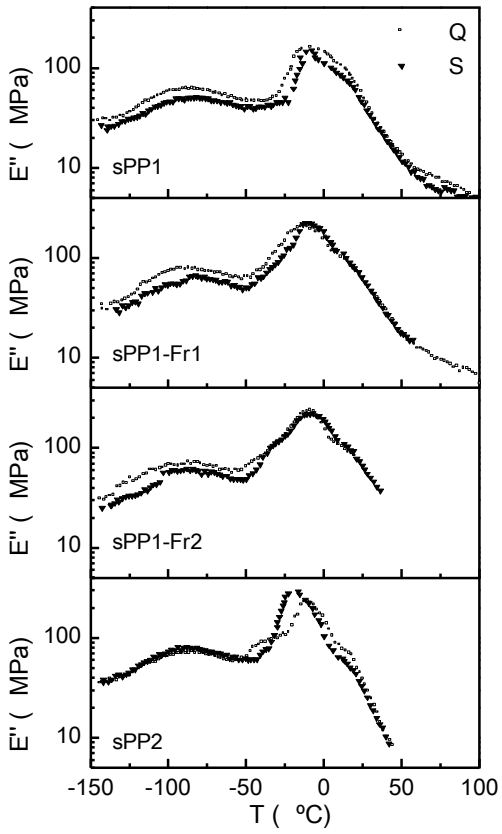

Fig. 9. Temperature-dependent variation of E'' for the different sPP samples at 3 Hz.

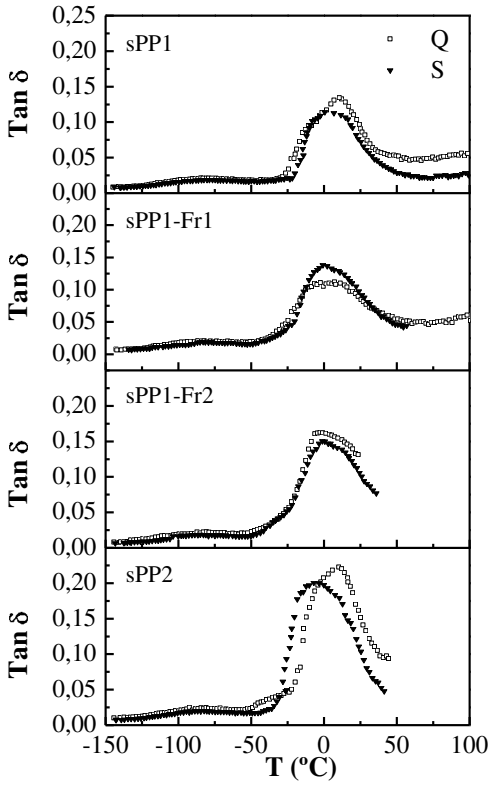

Fig. 10. Temperature-dependent variation of tan δ for the different sPP samples at 3 Hz.

As it was argued, the improvement of the crystals' quality through the S processing is expected to proceed in concurrence with the segregation of chains which breaks away from crystals. This separation process yields a more neat amorphous phase where motions occur without the restrictions imposed by crystals. Consequently, the observed diminution and increase of T_γ and E_{act} respectively in S-processed samples (Table 6) could reflect a local sub-T_g dynamics taking place at lower temperatures and likely involving a higher number of monomer units.

Tab. 4. Relaxation temperatures at 3 Hz and apparent E_{act} values calculated from E'' DMTA curves for the sPP samples.

Samples	Tγ (ºC)	$T^{'g}_{\beta}$ (ºC)	E_{act} γ (KJ/mol)	E_{act} β (KJ/mol)
sPP1-Q	-86	-11	55	250
sPP1-S	-89	-8.5	59	>400
sPP1-Fr1-Q	-76	-12	84	362
sPP1-Fr1-S	-81	-10	119	312
sPP1-Fr2-Q	-84	-11	103	>400
sPP1-Fr2-S	-93	-8	313	>400
sPP2-Q	-90	-10	55	250
sPP2-S	-87	-18	110	>400

Experimental part

Preparation of samples

Syndiotactic polypropylene samples were synthesized in a stainless steel autoclave designed and built in our laboratory. The syndiospecific catalyst $Ph_2C(Cp)(9\text{-}Flu)ZrCl_2$ (Boulder Scientific) used assures that the sPP samples prepared are free from any regiodefect arising from propylene mis-insertions (32). Methylaluminoxane (MAO) (Aldrich, 10% solution in toluene) was used as co-catalyst. The control of the reaction temperature allowed obtaining two polymers with different molar masses and syndiotacticity, sPP1 and sPP2. The reaction conditions are shown in Table 5. The sPP1 sample was fractionated by the method of successive extractions by increasing the temperature in a suitable solvent (33,34). The separation of the different fractions takes place according to their molar masses and steroregularities. Table 6 displays the conditions for the successive fractionation steps performed. Among the fractions obtained, the soluble fraction in xylene at 100 ºC, sPP1-Fr1, and the insoluble fraction in xylene at 120 ºC, sPP1-Fr2, have been chosen. The latter was yielded as a powdery sample by dissolving the compact residue in decaline at 140 ºC and precipitating with acetone. All samples were washed with acetone and dried in vacuum at room temperature.

Tab. 5. Polymerization conditions.

Sample	[Al/Zr]	T (ºC)	P (bar)	t (min)	weight (g)	[P] (mol/l)	Activity Kg pol/(mol Zr▪h▪mol P)
sPP1	813	20	2.0	90	6.2	2.0	6220
sPP2	813	60	2.0	30	7.2	0.5	109241

Tab. 6. Fractionation conditions from sPP1

Step	Solvent	V (mL)	t (h)	T (ºC)	Soluble Fraction	Insoluble fraction
0	-	-	-	-	sPP1	
1	Heptane	400	6	40	-	-
2	Heptane	400	7	60	-	-
3	Heptane	400	9	80	-	-
4	Xylene	400	7.5	100	sPP1-Fr1	-
5	Xylene	400	5	120	-	sPP1-Fr2

Characterization

The tacticity of the sPP2 sample was determined by ^{13}C-NMR analysis of a solution of the polymer in deuterated tetrachloroethane (70mg/1mL) at 80 ºC using a Innova 400 spectrometer. In the case of sample sPP1 and their fractions sPP1-Fr1, sPP1-Fr2, the ^{13}C-NMR spectra were obtained from 1,2,4-trichlorebenzene solutions in a **Bruker** Avance DPX-300 at 100 ºC and using deuterated o-dichlorobenzene as an internal reference. An acquisition time of 1 s, a relaxation delay of 4 s and a pulse angle of 45º were used. Table 1 shows the absolute configuration of the sPP samples at the pentad level.

The molar mass was estimated by means of the intrinsic viscosity in decaline stabilised with Irganox 1010 (1g/L) at 135 ºC (Table 1).

Processing

The polymers were compression-moulded to obtain films, which were subsequently used in the study of thermal and mechanical properties. A P-200-P Collins programmable compression moulding machine was used and a two-step processing was carried out. First, before running the final processing conditions, the material was homogenised by performing several open-close pressing cycles at 5 bar and 20 ºC above the melting temperature of the sample. Finally, the selected conditions (5 bar, T_m + 20 ºC) were applied for 5 min.

As far as the final cooling step is concerned, two procedures were performed: first, a rapid cooling from the melt between water-refrigerated plates, at 5 bar, for 7 min (Q processing). Second, a slow cooling from the melt without refrigeration, at 5 bar, down to room temperature (S processing). In all cases the films were annealed at room temperature for 24 h before performing any analysis.

Thermal analysis. DSC

The thermal properties were analysed in a Perkin-Elmer DSC-7 calorimeter connected to a cooling system and calibrated with Indium and Zinc. The samples, either Q or S, were studied in the -45 ºC to 190 ºC range. They were melted for a first time, followed by a dynamic crystallization and finally melted again to study the influence of the thermal history. The sample weight ranged from 2 to 5 mg. Both heating and cooling scanning rates used were 20 ºC/min. The T_g was determined as the temperature where the specific heat increment is half of the total change associated to the glass transition. The values of both T_m and T_c were taken respectively from the maximum and minimum of the peaks corresponding to these transitions.

WAXD analysis

Wide-angle X-ray diffraction (WAXD) patterns were recorded in the reflection mode by using a Bruker D8 Advance diffractometer provided with a Goebel mirror and a Vantec PSD detector. CuKα radiation was used, operating at 40 kV and 40 mA. The diffraction scans were collected at room temperature on samples either as a powder or as 2x2cm^2 square films. Additionally, two samples were chosen to monitor the time evolution of the WAXD pattern at selected temperatures. In particular, the crystalline growth of samples sPP1-FR2 and sPP2-Q were studied at 125 ºC and at room temperature, respectively. In the first case, an Anton-Paar TTK-450 chamber was employed as temperature controller. The WAXD crystallinity has been determined by subtraction of the corresponding amorphous component, by using the amorphous profile obtained at initial times. This initial WAXD profile in the case of the sPP2-Q film was taken as the amorphous halo for the calculation of the crystalline contents of the S and Q films.

Dynamic mechanical analysis. DMTA

Viscoelastic properties were measured with a Polymer laboratories MK II dynamic mechanical analyzer working in tensile mode. The temperature dependence of the storage modulus (E'), loss modulus (E''), and loss tangent (tan δ) was measured at 1, 3, 10 and 30 Hz over a temperature range from -140 ºC to 140 ºC at a heating rate of 1.5 ºC/min. The specimens used were rectangular films 2.2 mm wide, 100-250 μm thick and 17 mm long, obtained by compression moulding. The apparent activation energy values of the β and γ relaxations (E_{act}) were calculated according to an Arrhenius-type equation, from the frequency-dependent variation of the temperature at which E'' is maximum. The frequency dependence of the temperature associated to the maximum of the glass transition has been also considered to follow an Arrhenius behaviour, although it is due to cooperative motions. This approximation can be made without a significant error, since the interval of analyzed frequencies is short enough to be fitted to such a linear relationship.

Acknowledgements

The financial support of MICINN (Projects MAT2007 65519-C02-01, PET2008-0108 and MAT2010 19883) is gratefully acknowledged. We also thank the assistance of M.C. Martínez of Repsol in the ^{13}C NMR experiments.

References

[1] Natta, G.; Pasquon, I.; Zambelli, A. *J. Am. Chem. Soc.* **1962**, 84, 1488.
[2] Ewen, J. A.; Jones, R. L.; Razavi, A.; Ferrara, J. D. *J. Am. Chem. Soc.* **1988**, 110, 6255.
[3] De Rosa, C.; Auriemma, F. *Macromol. Symp.* **2001**, 175, 215.
[4] Rodriguez-Arnold, J.; Bu, Z.; Cheng, S. Z. D. *J. Macromol. Sci. Rev. Macromol. Chem. Phys.* **1995**, C35, 117.
[5] Lotz, B.; Mathieu, C.; Thierry, A.; Lovinger, A. J.; De Rosa, C. *Macromolecules* **1998**, 31, 9253.
[6] Napolitano, R.; Pirozzi, B. *Polymer* **1997**, 38, 4847.
[7] Guadagno, L.; D'Arienzo, L.; Vittoria, V. *J. Macromol. Sci. Phys.* **2000**, B39, 425.
[8] Guadagno, L.; D'Aniello, C.; Vittoria, V. *Macromolecules* **2000**, 33, 6023.

[9] Guadagno, L.; D'Aniello, C.; Gorrasi, G.; Naddeo, C.; Vittoria, V. *J. Macromol. Sci. Phys.* **2002**, B41, 289.
[10] [10a] De Rosa, C.; Auriemma, F.; Vinti, V. *Macromolecules* **1998**, 31, 7430. [10b] *Macromolecules* **1998**, 31**,** 6206.
[11] Auriemma, F.; Ruiz de Ballesteros, O.; De Rosa, C. *Macromolecules* **2001**, 34, 4485.
[12] De Rosa, C.; Gargiulo, M. C.; Auriemma, F.; Ruiz de Ballesteros, O.; Razavi, A. *Macromolecules* **2002**, 35, 9083.
[13] Auriemma, F.; De Rosa, C. *J. Am. Chem. Soc.* **2003**, 125, 13143.
[14] Auriemma, F.; De Rosa, C. *Macromolecules* **2003**, 36, 9396.
[15] De Rosa, C.; Auriemma, F.; Ruiz de Ballesteros, O.; Resconi, L.; Fait, A.; Ciaccia, E. *J. Am. Chem. Soc.* **2003**, 125, 10913.
[16] De Rosa, C.; Auriemma, F.; Ruiz de Ballesteros, O. *Macromolecules* **2003**, 36, 7607.
[17] De Rosa, C.; Corradini, P.; *Macromolecules* **1993**, 26, 5711.
[18] De Rosa, C.; Auriemma, F. *Prog. Polym. Sci.* **2006**, 31, 145.
[19] De Rosa, C.; Auriemma, F.; Vinti, V. *Macromolecules* **1997**, 30, 4137.
[20] Struik, L. C. E. *Physical Aging of Amorphous Polymers and other Materials*, Elsevier, Amsterdam, **1978**.
[21] Petrie, S. E. B. *J. Macromol. Sci. Phys.* **1976**, B12, 225.
[22] Haftka, S.; Könnecke, K. *J. Macromol. Sci. Phys.* **1991**, B30, 319.
[23] Bond, E. B.; Spruiell, J. E.; Lin, J. S. *J. Polym. Sci. Part B Polym. Phys.* **1999**, 37, 3050.
[24] Wunderlich, B. *Macromolecular Physics*, Academic Press , New York, **1980**.
[25] Krache, R.; Benavente, R.; López-Majada, J. M.; Pereña, J. M.; Cerrada, M. L.; Pérez, E. *Macromolecules* **2007**, 40, 6871.
[26] McCrum, N. G.; Read, B. E.; Williams, G. *Anelastic and Dielectric Effects in Solid Polymers*, Dover, New York, **1991**.
[27] Bartenev, G. M.; Aliguliev, R. M. *Polym. Sci. USSR.* **1984**, 26, 1383.
[28] Men, Y.; Strobl, G. *Polymer* **2002**, 43, 2761.
[29] Arranz-Andrés, J.; Guevara, J. L.; Velilla, T.; Quijada, R.; Benavente, R.; Pérez, E.; Cerrada, M. L. *Polymer* **2005**, 46, 12287.
[30] Jourdan, C.; Cavaille, J. Y.; Pérez, J. *J. Polym. Sci. Part B Polym. Phys.* **1989**, 27, 2361.
[31] Zhang, X.; Zhao, Y.; Wang, Z.; Zheng, C.; Dong, X.; Su, Z.; Sun, P.; Wang, D.; Han,C.; Xu, D. *Polymer* **2005**, 46, 5956.
[32] Longo, P.; Proto, A.; Grassi, A.; Ammendola, P. *Macromolecules* **1991**, 24, 4624.
[33] Cantow, M. J. R. *Polymeric Frationation*, Academic Press, New York **1996**.
[34] Tung, H. L. *Fractionation of Synthetic Polymers, Principles and Practices*, Marcel Dekker, New York, **1997**.